The Highly Effective Cobalt Based Metal–Organic Frameworks Catalyst for One Pot Oxidative Esterification Under Mild Conditions

Pagasukon Mekrattanachai[1] · Lei Zhu[2,3] · Naruemon Setthaya[1] · Chakkresit Chindawong[1] · Wei Guo Song[2,3]

Abstract

The cobalt-based metal organic frameworks (Co-MOFs) catalyst has been prepared with using terephthalic acid and 4,4′-bipyridine as organic linkers by facile solvothermal method for one pot oxidative esterification. The prepared catalyst was pyrolysed at different temperature and then applied for oxidation of aldehyde using molecular oxygen as benign oxidant under mild conditions. The Co-MOFs pyrolysed at 800 °C (denoted as Co-MOFs-800) catalyst exhibited excellent catalytic activity, selectivity and recyclability toward the oxidative esterification of benzaldehydes. Furthermore, it can be reused up to 5 runs without significant loss of activity.

Graphic Abstract
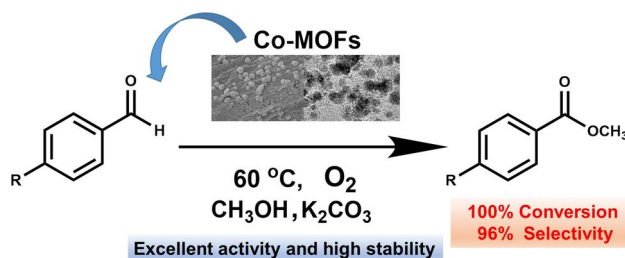
1 Introduction

The direct synthesis of esters from the oxidation of aldehydes is an important transformation in organic synthesis due to these compounds find extensive applications in the synthesis of various natural and bioactive products [1–3]. The conventional method for the synthesis of esters involves the reaction of carboxylic acids or acid derivatives (acid chlorides and anhydrides) with alcohols, which is a multistep process and often leads to the formation of large amounts of waste and undesired by-products [4, 5]. In the recent years, direct catalytic transformation of alcohol or aldehydes to esters, without using acid or acid-derivative has gained considerable interest. Currently, a number of various kinds heterogeneous catalysts for oxidative esterification to the corresponding esters have been reported in the literatures. However, most of the reported

✉ Pagasukon Mekrattanachai
pagasukon.me@up.ac.th

✉ Wei Guo Song
wsong@iccas.ac.cn

1 School of Science, Department of Chemistry, University of Phayao, 19 Moo 2 Tambon Maeka Amphur, Mueang Phayao 56000, Thailand

2 Beijing National Laboratory for Molecular Sciences, Laboratory of Molecular Nanostructures and Nanotechnology, CAS Research/Education Center for Excellence in Molecular Sciences, Institute of Chemistry, Chinese Academy of Sciences, Beijing 100190, China

3 University of Chinese Academy of Sciences, Beijing 100049, China

catalysts are based on noble metals such as Au, Ag, Pd, including bimetallic Au–Ag on supporting materials [6–16]. These catalysts are not only expensive, but they also involve the multistep synthetic procedures. Therefore, the development of non-noble metal heterogeneous catalyst with cost-effective and high efficiency is a great attractive for oxidative esterification.

Transition metal nanoparticles (NPs) especially Co, Cu, Ni, Fe etc. supported on N doped carbon material are extraordinarily active non-precious metal catalysts for green, economic and sustainable catalytic process [17–19]. In particular, Co NPs based carbon materials (Co@NC) are found to be the powerful catalysts for oxidative esterification because there are two potential catalytic active sites consisting of Co NPs and Co–N_x sites in Co@NC [20–24]. Generally, the common procedure for preparation of Co NPs based carbon materials is wetness impregnation of carbon materials (carbon black or carbon nanotube) with Co(II)complex or Co(II) ion precursor, followed by pyrolysis at 800 °C under inert gas [25–27]. Another facile method is the carbonization of cobalt-nitrogen containing metal organic frameworks (MOFs) such as ZIF-67 at temperatures in the range of 600–900 °C to ensure the formation of Co–N doped graphitic material [28–30].

Metal–organic frameworks (MOFs), an important class of crystalline porous materials, have received growing interest for catalytic application [31–34]. MOFs are solids with permanent porosity which are built from nodes (metal ions or clusters) coordinated with organic bridging linkers to form well organized coordination networks. [35, 36]. The most significant feature of MOFs is their potential inner porosity and that guest molecules can access the pores which are important for catalytic purposes. A well known zeolite-type cobalt-organic frameworks (Co-MOFs), ZIF-67 with 2-methylimidazole as organic linker is widely investigated in several catalytic system such as Fenton-like catalysis [37], pollutant photodegradation [38, 39], hydrogenation [40–42], epoxidation [43]. It is also applied for oxidative esterification [44–47], and showed the high activity. However, the investigation of Co-MOFs with other organic linkers are still rare for organic transformation.

Herein, the cobalt-organic frameworks (Co-MOFs) with using terephthalic acid and 4,4′-bipyridine as organic linkers were prepared and studied in oxidative esterification under O_2 molecule as green oxidizing agent. Based on our knowledge, this is the first time to apply this catalyst for oxidative esterification reaction. The developed Co-MOFs catalyst has several advantages such as the use of a low cost metal, high stability and excellent catalytic activity. Furthermore, good magnetization of the synthesized catalyst allowed it to be readily separated from the reaction mixture by using external magnet.

2 Experimental Section

2.1 Preparation of Co-Metal–Organic Frameworks

In this work Co-metal–organic frameworks catalyst was prepared with a modified method using the mixed solvent between DI water and dimethylformamide or DMF (1:1 v/v) as solvent [48–52]. In a typical synthesis, $Co(NO_3)_2 \cdot 6H_2O$ (3.75 mmol) was dissolved in the mixed solvent of DI water and DMF (20 mL) to form a clear solution. Then terephthalic acid (3.75 mmol) in mixed solvent (20 mL) was added by NaOH (7.5 mmol) in 5 mL DI water yielding clear solution. Another linker, 4,4′-bipyridine (3.75 mmol) in mixed solvent (20 mL) was also prepared. After that, the terephthalic acid and 4,4′-bipyridine solutions were added into Co(II) solution and the mixture was stirred for 5 min. The mixture was transferred into Teflon-lined autoclave and then heated at 120 °C for 12 h. The powder was separated by centrifugation, washed by DMF, DI water, and dried at 100 °C for overnight. Finally, the powder was pyrolysed at high temperature (600, 700, 800 and 900 °C) for 3 h. under Ar gas (100 mL/min, 2 °C/min).

2.2 Characterization

Powder X-ray diffraction (XRD) patterns of the samples were recorded with D8 Advance, Bruker using Cu-Kα radiation with wavelength 1.5418 Å, 40 kV, 40 mA. The cobalt contents in the samples were measured quantitatively by inductively couple plasma atomic emission spectroscopy (ICP-AES; IPPE-9000, Shimadzu Plasma Atomic Emission Spectrometer). The surface morphology of the materials was investigated using a scanning electron microscope (FESEM, JEOL-6701F electron microscope). The structure and the elemental distribution were determined using a high resolution transmission electron microscope (TEM, JEOL 2100F electron microscope). The BET surface area and pore size were measured using N_2 adsorption/desorption isotherms at 77 K on a BET Micromeritics ASAP 2460. X-ray photoelectron spectroscopy (XPS) was performed by using an ESCALab220i-XL electron spectrometer. The basicity of the prepared catalysts were examined by CO_2-TPD analysis. Temperature programmed desorption (TPD) was carried out by using CO_2 as the probe molecule. Sample was pre-treated in He flow at 300 °C for 60 min and cooled to room temperature. After being saturated with CO_2, the sample was purged with He for 40 min at room temperature to sweep the physical molecule. Then sample was heated by 600 °C at the rate of 10 °C/min. The signals were monitored by a thermal conductivity detector (TCD). The elemental content (C, N

and O) of the prepared catalysts were also determined by energy dispersive spectroscopy (EDS) technique in conjunction with TEM.

2.3 Oxidative Esterification of Benzaldehyde and Benzaldehyde Derivative

The Co-metal–organic frameworks catalyst (20 mg), alcohol, benzaldehyde or benzaldehyde derivatives (1 mmol), methanol (5 mL) and K_2CO_3 (0.5 mmol) were charged into a reaction vessel equipped with a magnetic stirring bar. The vessel was evacuated and agitated under 0.5 or 1 MPa of O_2, then the mixture was heated to 60 °C for the desired reaction time. After the completion of reaction, the catalyst was separated by centrifugation and the filtrate was determined by GC-FID (Shimadzu GC-2010-Plus) and GC-MS (Shimadzu GCMS-QP2010) by using chlorobenzene as internal standard.

2.4 Reusability Test

The recyclability of the Co-metal–organic frameworks catalyst was tested for oxidative esterification maintaining the same reaction conditions as described above, except the reaction was scaled up by factor 2. The Co-metal–organic frameworks catalyst (40 mg), benzaldehyde (2 mmol), methanol (10 mL) and K_2CO_3 (1 mmol) were charged into a reaction vessel equipped with a magnetic stirring bar. The

vessel was evacuated and agitated under 1 MPa of O_2, then the mixture was heated to 60 °C for 3 h. Then, the catalyst was separated by centrifugation, thoroughly washed with methanol (3 × 10 mL) and dried at 90 °C overnight. After that, it was reused for a consecutive reaction with fresh benzaldehyde and methanol.

3 Results and Discussion

## 3.1 Characterization of the Prepared Catalysts

The phase of prepared Co-MOFs sample has been confirmed by powder X-ray diffraction (XRD). Upon thermal treatment at different temperatures, all XRD patterns showed three peaks characteristic of metallic Co (JCDPF-15-0806) [38], the intensity of which gradually increased along with elevated annealing temperature, revealing the improved crystallinity of metallic Co and its significant effect with annealing temperature (Fig. 1).

The morphology of the prepared Co-MOFs catalysts were studied by SEM and TEM techniques (Figs. 2 and 3). The SEM and TEM images for the Co-MOFs pyrolysed at 600–800 °C obviously showed the regular distribution of Co nanoparticles. The particles size of all samples were also determined, and the larger particles size was observed with the increased pyrolysis temperature from 600 to 900 °C (Fig. 3). The distribution of Co nanoparticles is uniform with

Fig. 1 XRD patterns of Co-MOFs catalysts which were pyrolysed at 600, 700, 800 and 900 °C for 3 h. under Ar gas
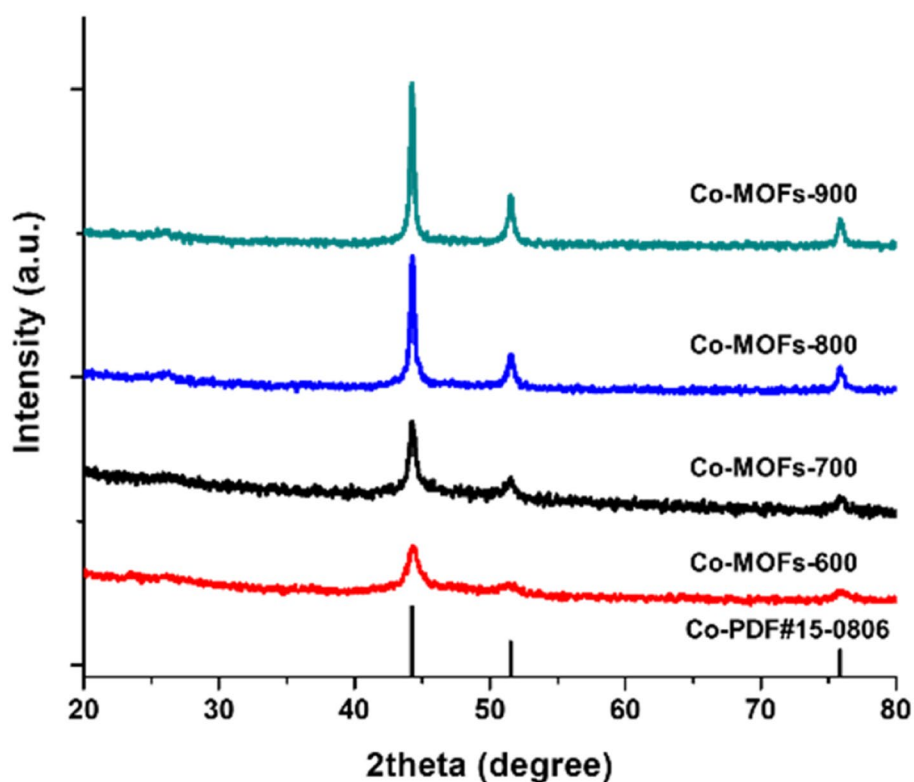
Fig. 2 SEM images of Co-MOFs catalysts pyrolysed at 600, 700, 800 and 900 °C for 3 h under Ar gas
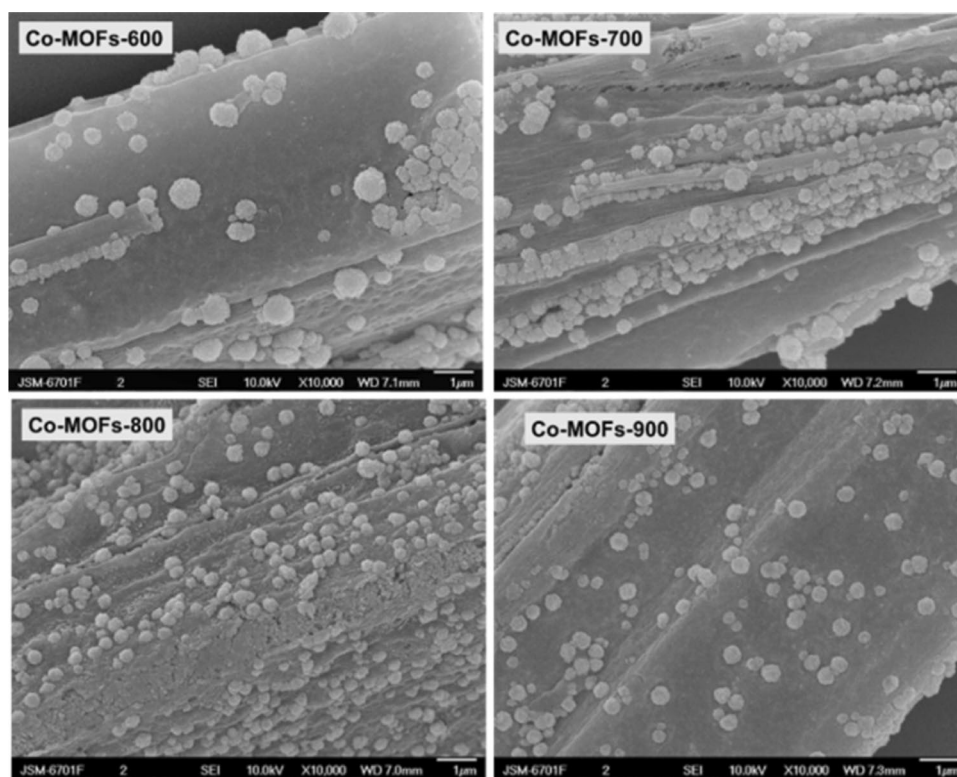
the sizes of about 5.31, 7.50 and 7.61 nm, for the Co-MOFs pyrolysed at 600, 700 and 800 °C respectively. While the size of Co nanoparticles pyrolysed at 900 °C were increased rapidly to about 47.96 nm and the distribution of Co nanoparticles was not uniform. This might be due to the aggregation of Co nanoparticles at high pyrolysis temperature. The Co size distribution results indicated that pyrolysis temperature plays an important role in the dispersion of metallic Co particles. And the higher pyrolysis temperature, the higher Co loading was obtained because the more ligands of MOFs could decompose at high temperature (Table S1, in the Supporting Information). However, due to the high Co metal content, partial particle agglomeration is occurred, especially at high calcination temperature. The high-resolution TEM (HRTEM) images of all samples (Fig. S1, in the Supporting Information) unambiguously exhibited the two lattice fringes with lattice spaces of 0.35–0.36 nm and 0.18–0.21 nm, corresponding to the graphitic layer domains and the crystalline Co nanoparticle, respectively [39, 53]. This indicates the high crystallinity of the Co-MOFs samples. The element mapping of Co-MOFs-800 was also shown in Fig. 4 and it demonstrated the co-existence and homogenous dispersion of Co, C, O and N species.

All N_2 adsorption-desorption isotherms of all Co-MOFs catalysts were close to type-IV with a hysteresis loop (Fig. 5) [52]. The Co-MOFs calcined at 600 and 800 °C showed the slightly higher BET surface area than the others and their pore sizes were in the range of 7.57–11.72 nm (Table S1 in the Supporting Information).

To gain further insight into the catalyst structure, X-ray photoelectron spectroscopy (XPS) characterization was performed on the samples. In the cobalt region of Co-MOFs samples, peaks characteristic of metallic Co were observed with the typical binding energies of 794.03 and 778.05 eV, assigned to Co $2p_{1/2}$ and Co $2p_{3/2}$ electrons of Co metal, respectively (Fig. 6) [43, 54, 55]. Moreover, a dominant peak of Co-MOFs samples annealed at 800 and 900 °C catalysts were obviously seen at 779.06 eV, which should be ascribed to N-coordinated metal (Co–N_x) [56, 57]. For Co-MOFs-600 and Co-MOFs-700 samples, the low intensity of this peak was observed. The XPS spectra of C1s for all samples (Fig. S3, in the Supporting Information) showed the binding energy that can be assigned to C–C units at 284.5 ± 0.3 eV, and C=O units at 288.5 ± 0.4 eV [58]. In addition, the N 1s spectrum for Co-MOFs-800 catalyst exhibited main peak of pyridinic nitrogen with binding energy of 398.94 eV, confirming the coordination of nitrogen from 4,4′-bipyridine linker [55] (Fig.S2 in the Supporting Information). These results indicate that N atoms have been successfully embedded in the carbon matrix, and some of them might associate with the Co species to form Co–N_x sites, which play an important role in oxidative esterification.

Base on the above results, metallic Co supported N-doped carbon derived from Co-MOFs (Co@NC) was successfully

Fig. 3 TEM images with their sizes distribution of Co-MOFs catalysts pyrolysed at 600, 700, 800 and 900 °C for 3 h under Ar gas
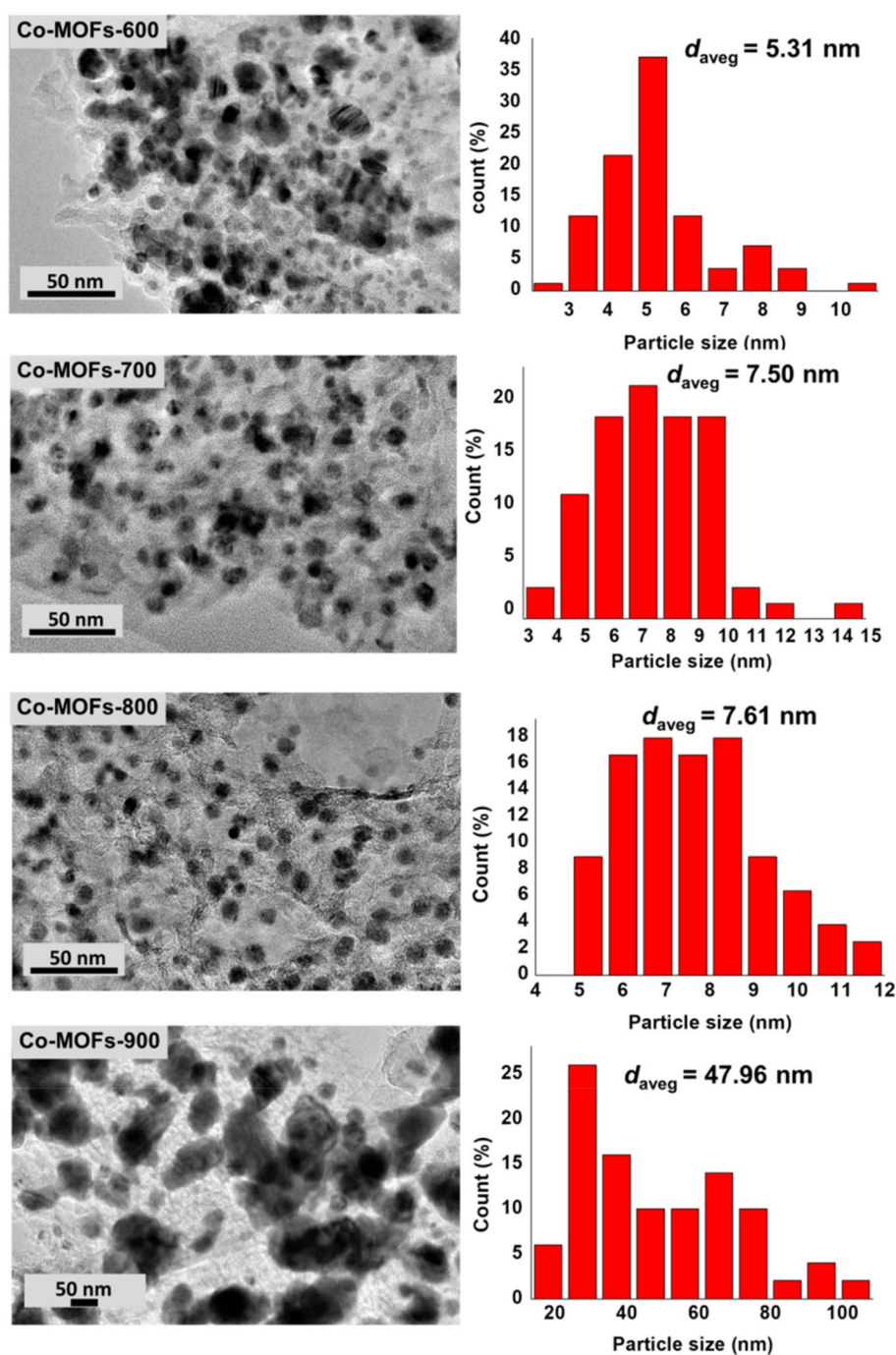

prepared by carbonization of Co-MOFs at high temperatures under inert gas.

Moreover, the relationship between basicity and catalytic activity was investigated. CO_2-TPD was employed to examine the basicity of Co-MOFs pyrolysed at 600–900 °C and the results were shown in Fig 7. For Co-MOFs catalysts pyrolysed at 600, 700 and 800 °C, the peaks of strong basic sites between 400 and 500 °C were observed. And the small peak of weak basic site between 350 and 400 °C were also observed for Co-MOFs-600 sample. On the other hand, Co-MOFs-900 catalyst exhibited only peak of weak basic site, and the amounts of basic sites for Co-MOFs-600, Co-MOFs-700, Co-MOFs-800 and Co-MOFs-900 were 1.30, 1.83, 1.87 and 1.13 mmol/g, respectively. These results indicated that the decrease of the amounts of strong basic sites contributed to the declined of the catalysts [59–61].

Fig. 4 HRTEM images of Co-MOFs-800 catalyst and EDS mapping
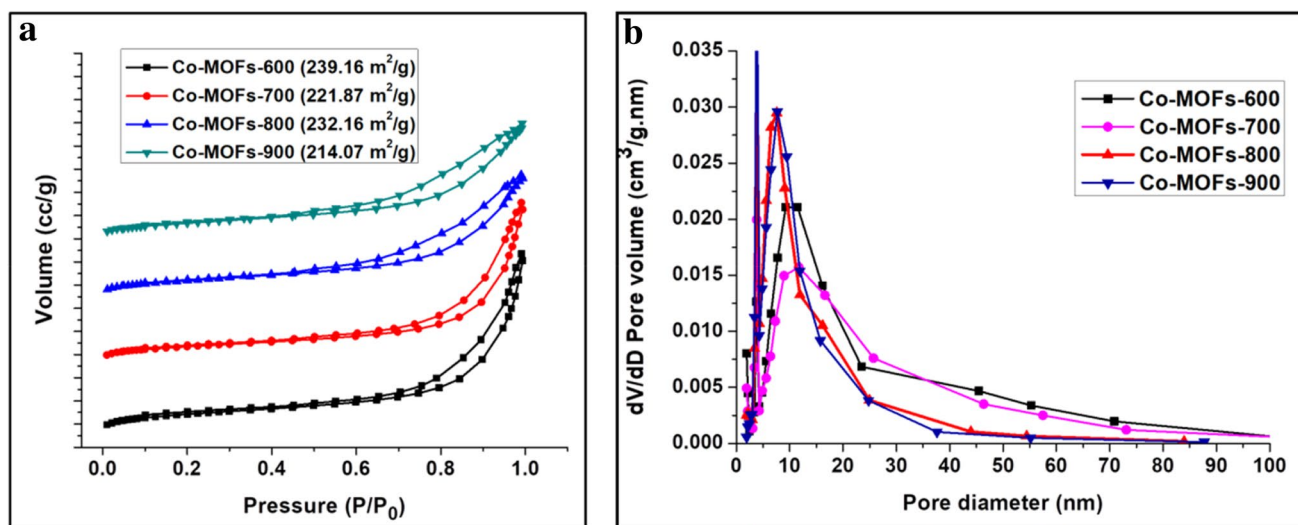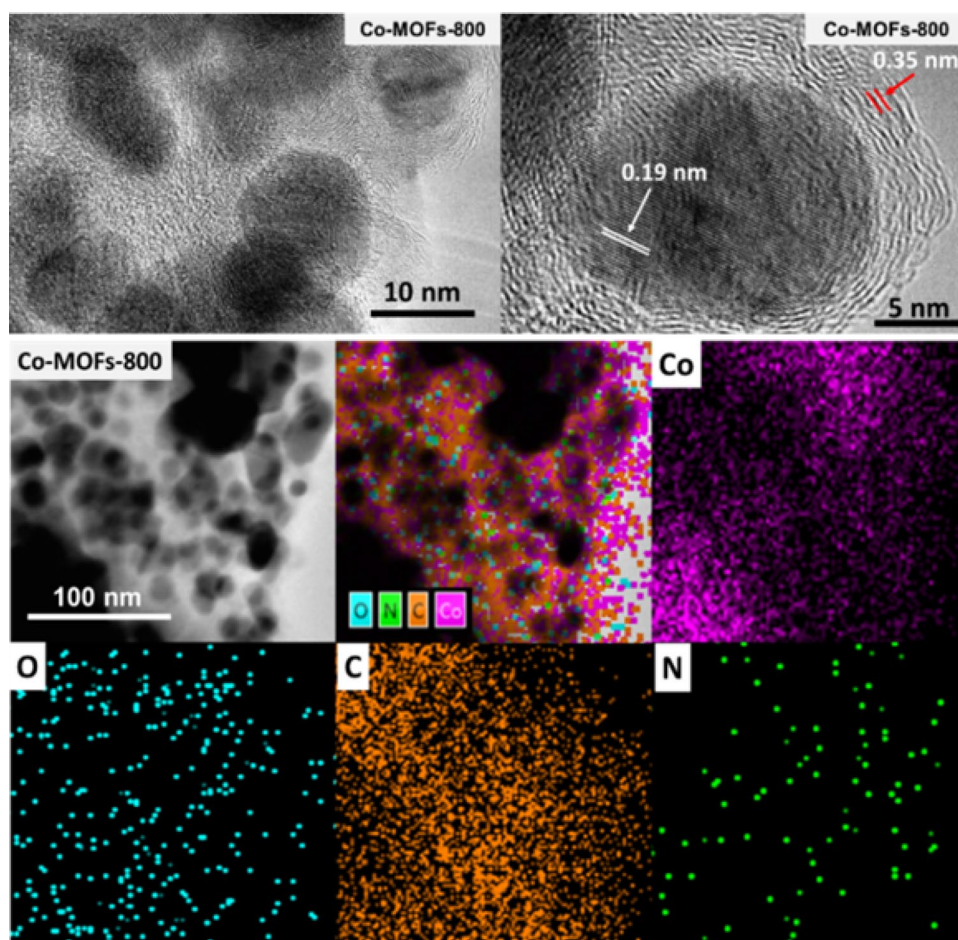
Fig. 5 **a** N$_2$ adsorption–desorption isotherms and **b** pore size distribution of Co-MOFs catalysts pyrolysed at 600, 700, 800 and 900 °C for 3 h under Ar gas
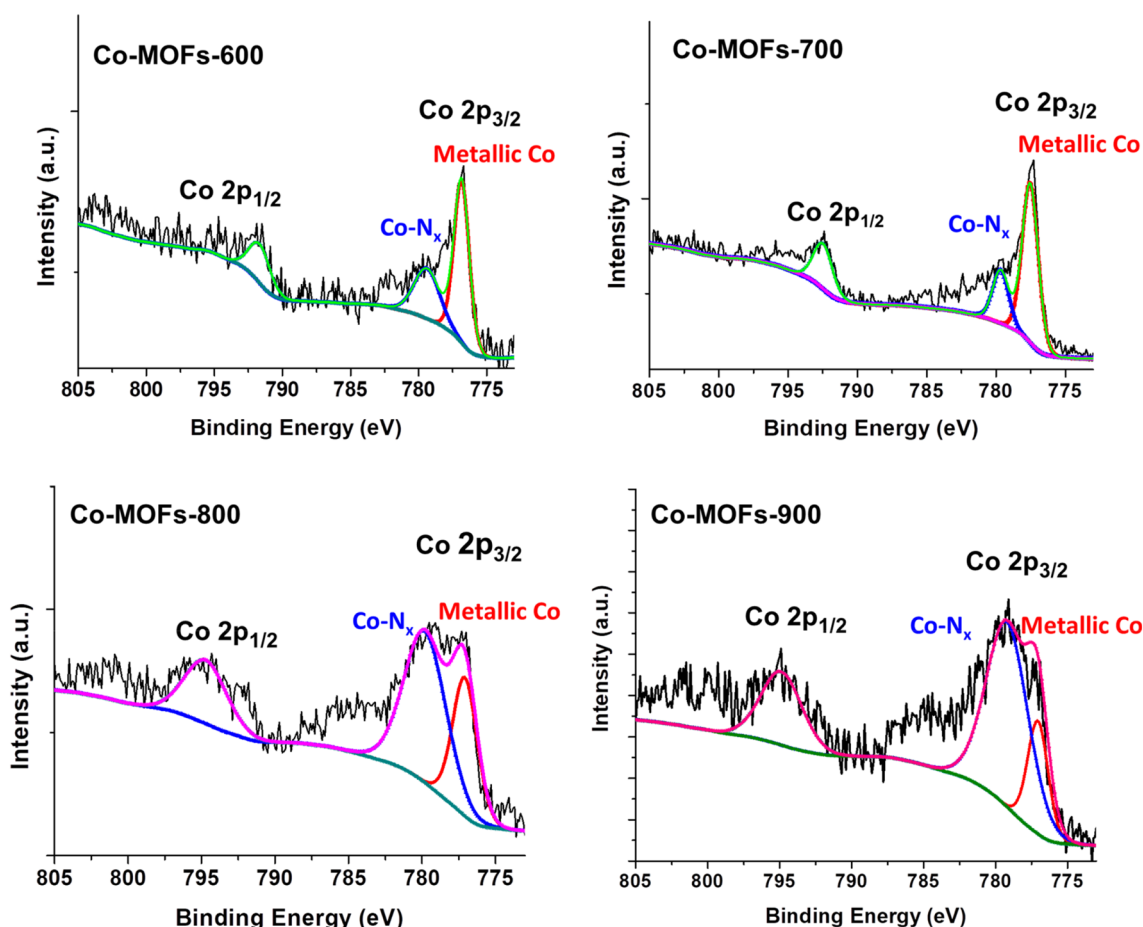
Fig. 6 XPS analysis of Co-MOFs catalysts which were pyrolysed at 600, 700, 800 and 900 °C for 3 h under Ar gas
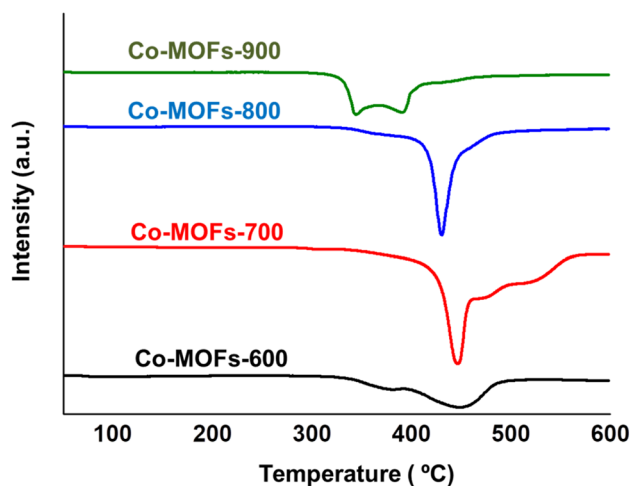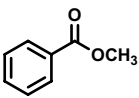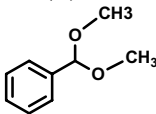

Fig. 7 CO_2-TPD profiles of Co-MOFs-600, Co-MOFs-700, CoMOFs-800 and Co-MOFs-900 catalysts

3.2 Catalytic Activity

The catalytic activity of the synthesized Co-MOFs catalysts was tested for the oxidative esterification of benzaldehyde and benzylic alcohol with methanol to give methyl benzoate. Typically, the model reaction was performed at 60 °C using oxygen molecule as an oxidant in the presence of K_2CO_3 as base. After finishing the reaction, the catalyst powder was removed by centrifugation, and then the filtrate was determined by GC-FID and GC-MS by using chlorobenzene as internal standard to confirm the obtained products. As a result, the main peak of methyl benzoate was observed and the another was (dimethoxymethyl)benzene or acetal byproduct. The results of the optimization experiments were summarized in Table 1. As can be seen, Co-MOFs calcined at 800 °C (denoted as Co-MOFs-800) showed the best activity and selectivity to the only targeted product within 12 h (entry 3). For comparison, the prepared catalyst with different pyrolysis temperatures showed lower activity or/and selectivity to varying extents (entries 1-4). This indicated that the higher Co content in the high pyrolysed temperature catalyst,

Table 1 Oxidative esterification of benzaldehyde and methanol over Co-MOFs catalysts which were pyrolysed at different temperatures

Entry	Catalyst	O_2 Pressure (MPa)	Time (h)	Conv. (%)	Sel. (%)	Sel. (%)
1	Co-MOFs-600	1	12	66	51	49
2	Co-MOFs-700	1	12	74	79	21
3	Co-MOFs-800	1	12	100	96	4
4	Co-MOFs-900	1	12	96	92	8
5	Co-MOFs-800	1	9	100	83	17
6	Co-MOFs-800	1	6	94	72	28
7	Co-MOFs-800	0.5	12	96	94	6
8	Co-MOFs-800[a]	0.5	12	81	99	1
9	Co-MOFs-800[b]	1	12	75	1	99
10	Co-MOFs-800[b]	1	24	85	1	99
11	No catalyst	1	24	10	3	97

Reaction conditions: Co-MOFs catalyst (20 mg), benzaldehyde (1 mmol), methanol (5 mL), K_2CO_3 (0.5 mmol), 60 °C reaction temperature

[a] Amount of Co-MOFs-800 was 10 mg

[b] Without base

the higher catalytic activity was observed and the optimized Co loading in this experiment was 32.3 wt%. Although the Co content of the Co-MOFs catalysts pyrolysed at 900 °C is the highest (36.2 wt%), its catalytic activity was lower than that Co-MOFs catalyst pyrolysed at 800 °C. This might be due to the lowest basic sites in Co-MOFs-900, the aggregation and the large size of Co nanoparticles (47.96 nm). The Co-MOFs-800 catalyst was further tested at 0.5 MPa O_2. As a result, it also exhibited the excellent catalytic activity with 96% conversion and 94% selectivity of methyl benzoate (entry 7). The presence of base was demonstrated to be necessary for the conversion (entries 9–10). After having demonstrated the excellent activity of Co-MOFs-800 in the model reaction, a wide range of aldehydes containing electron donating as well as withdrawing groups were oxidized under described experimental conditions. The results were summarized in Table 2. All the substrates were smoothly oxidized to give the desired products with excellent catalytic performances. In general, aromatic aldehydes substituted with electron-withdrawing groups such as para-nitro, fluoro and bromo were found to be more reactive and afforded desired products with high selectivities of ester products than those containing electron donating groups and lower electronegativity groups (para-methoxy and chloro groups) [62]. For ortho-nitrobenzaldehyde (entries 6–7), the reactivities were lower than the others which owing to the steric effect of substrate structure, resulting the difficulty in the interaction between substrate and catalyst surface [63]. According to the XPS analysis shown above, the catalytic active centres in this prepared catalyst could be metallic Co NPs and Co–N_x
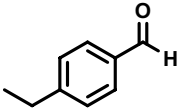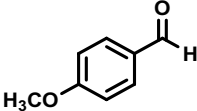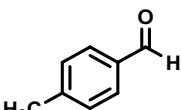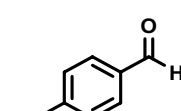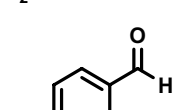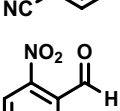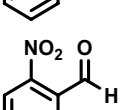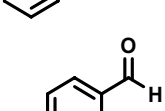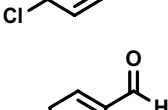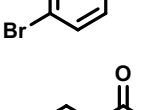
sites in this prepared catalyst, resulting the excellent catalytic activity of this catalyst for oxidative esterification of benzaldehyde. This correspond to the synergistic catalytic effect between Co–N_x sites and Co NPs in the previous literature [64].

The catalytic study was then extended to the oxidative esterification of various benzylic alcohols using the Co-MOFs-800 catalyst, and the results were summarized in Table 3. As a result, various benzylic alcohols were converted into the corresponding methyl esters in moderate to high conversions (53–96%). The benzylic alcohols substituted with electron donating groups (–OCH_3 and –CH_3) showed a higher conversions (entry 2 and 3) in comparison to benzylic alcohols substituted with electron withdrawing groups (–Br, –NO_2, –Cl). The aldehyde by-product was also observed in oxidative esterification of alcohol. Benzyl alcohol were oxidized to only benzaldehyde, when benzylic alcohols substituted with methoxy and methyl group were oxidized to desired esters with moderate selectivities (entry 2 and 3). On the other hand, benzylic alcohols substituted with –Br and –Cl group were oxidized to higher selectivities (entry 4 and 5). The –NO_2 substituted benzyl alcohol exhibited only 27% selectivity of ester product. According to this results, when alcohols were used as starting materials, they exhibited the lower catalytic activity in comparison to using aldehydes as starting materials. This might be due to the low coordination between hydroxyl group and active Co NPs or Co–N_x sites in the catalyst, therefore, the small amount of alcohol molecules could adsorb on catalyst surface.

Based on the above results and taking into the previous reports [8, 45, 65–67], the proposed reaction mechanism for

Table 2 Oxidative esterification of benzaldehyde derivatives and methanol over Co-MOFs-800 catalyst

Entry	Substrates	Time (h)	Conv. (%)	Sel. (%)
1	4-ethylbenzaldehyde	12	98	100
2	4-methoxybenzaldehyde (H₃CO)	12	84	91
3	4-methylbenzaldehyde (H₃C)	12	97	100
4	4-nitrobenzaldehyde (O₂N)	12	100	100
5	4-cyanobenzaldehyde (NC)	12	97	100
6	2-nitrobenzaldehyde (NO₂)	12	75	100
7	2-nitrobenzaldehyde (NO₂)	20	82	100
8	4-chlorobenzaldehyde (Cl)	12	85	100
9	4-bromobenzaldehyde (Br)	12	99	100
10	4-fluorobenzaldehyde (F)	12	96	100

Reaction conditions: Co-MOFs-800 catalyst (20 mg), benzaldehyde derivatives (1 mmol), methanol (5 mL), K_2CO_3 (0.5 mmol), O_2 (1 MPa), 60 °C reaction temperature

the oxidative esterification of benzaldehyde over metallic Co supported N-doped carbon derived from Co-MOFs (Co@NC) was illustrated in Scheme 1. According to the result in Table 1 (entry 11), the catalytic activity in the absence of catalyst was only 10% conversion and 3% selectivity of ester product, eventhough the reaction time was prolong to 24 h. Meanwhile, the much higher %conversions and %selectivities of ester product were obtained in the presence of catalyst. This indicated that, this prepared Co catalyst is essential for this reaction. Therefore, in the first step, the active Co–N_x sites in the catalyst could adsorb benzaldehyde through oxygen atom from carbonyl group, promoting the electrophilic properties of aldehydes, following nucleophilic attacking from methanol yielding hemiacetal species. Then, the hemiacetal intermediate transforms directly to an ester product over the catalyst surface with using O_2 as an oxidant. For this step the Co–N_x sites could capture the molecular O_2 under the assistance of the doped nitrogen to form metal alcoholate specie 1, then β-hydride elimination which is promoted by K_2CO_3, takes place to form the ester product. Meanwhile, further condensation between the hemiacetal and methanol can occur, and thus the acetal byproduct was also observed.
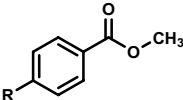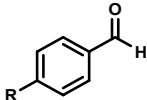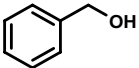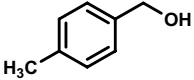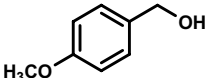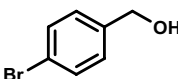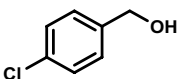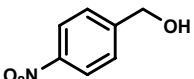
3.3 Reusability Test

To demonstrate the stability and reusability of Co-MOFs-800 catalyst, we have checked the recycling of the catalyst by using benzaldehyde as a model substrate. After completion of the reaction, the catalyst was easily recovered from reaction mixture by using external magnet, washed with methanol and then dried. The recovered catalyst was used for five subsequent runs under similar reaction conditions. The results of recycling experiments were shown in Fig. 8. The %selectivity of the methyl benzoate product remained in all cases. This confirmed that the developed catalyst was quite stable and could be reused efficiently without any significant loss in activity. Furthermore, the cobalt content in the recovered catalyst after the fifth run was found to be almost similar (31.6 wt%) as in the fresh catalyst (32.3 wt%) as determined by ICP-AES analysis. The XRD result and TEM images of the used catalyst was also similar to the fresh catalyst, confirming the high stable of our prepared catalyst (Figs. S4 and S5 in the Supporting Information)

4 Conclusions

The cobalt-based metal organic frameworks (Co-MOFs) catalyst has been prepared for the oxidative esterification using molecular oxygen as benign oxidant under mild conditions. The Co nanoparticles pyrolysed at different temperatures showed different catalytic activities. The Co-MOFs pyrolysed at 800 °C (denoted as Co-MOFs-800) exhibited superior catalytic activity toward the oxidative esterification of benzaldehyde and benzaldehyde derivatives to the corresponding methyl ester products, which is ascribed to the synergistic catalytic effect between Co NPs and Co–N_x

Table 3 Oxidative esterification of various alcohols and methanol over Co-MOFs-800 catalyst

Entry	Substrates	Time (h)	Conv. (%)	Sel. (%) methyl benzoate	Sel. (%) benzaldehyde
1	benzyl alcohol (OH)	24	53	0	100
2	4-methylbenzyl alcohol (H_3C)	24	78	78	22
3	4-methoxybenzyl alcohol (H_3CO)	24	96	55	45
4	4-bromobenzyl alcohol (Br)	24	50	82	18
5	4-chlorobenzyl alcohol (Cl)	24	54	100	0
6	4-nitrobenzyl alcohol (O_2N)	24	69	27	73

Reaction conditions: Co-MOFs-800 catalyst (20 mg), alcohol (1 mmol), methanol (5 mL), K_2CO_3 (0.5 mmol), O_2 (1 MPa), 60 °C reaction temperature

Scheme 1 Mechanism proposed for the oxidative esterification of benzaldehyde over metallic Co supported N-doped carbon derived from Co-MOFs (Co@NC)
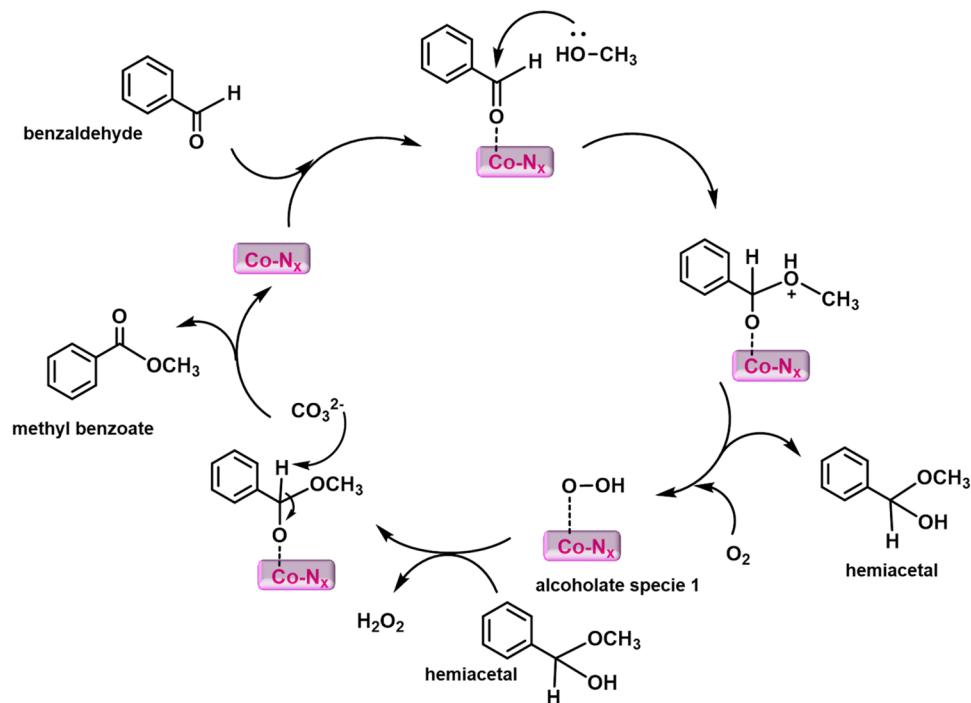
Fig. 8 Reusability of Co-MOFs-800 catalyst in the oxidative esterification of benzaldehyde. Reaction conditions: catalyst (40 mg), benzaldehyde (2 mmol), methanol (10 mL), K_2CO_3 (1 mmol), 60 °C, O_2 (1 MPa), 3 h reaction time
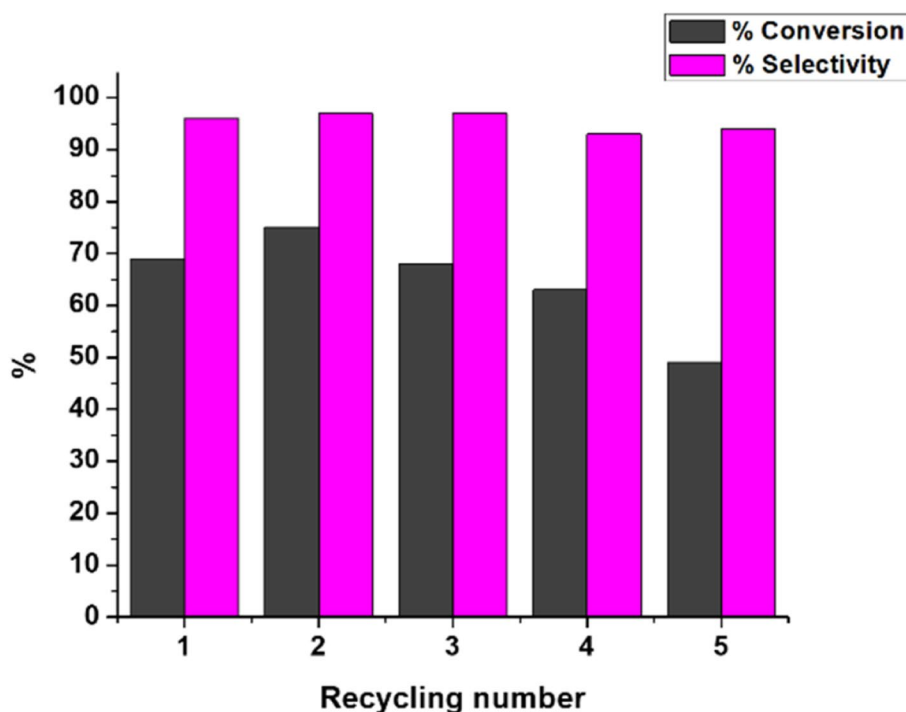
active sites in the prepared catalyst. Furthermore, our prepared Co-MOFs-800 catalyst could be reused at least five consecutive runs without significant loss of activity, confirming the high stability of this prepared catalyst.

Declarations

Conflict of interest There are no conflicts to declare.

References

1. Ogawa T, Matsui M (1976) J Am Chem Soc 98:1629–1630
2. Wilson SR, Tofigh S, Misra RN (1982) J Org Chem 47:1360–1361
3. Garegg PJ, Olsson L, Oscarson S (1995) J Org Chem 60:2200–2204
4. Otera J, Nishikido J (2010) Esterification; methods, reactions, and applications, 2nd edn. Wiley-VCH, Weinheim
5. Smith MB, March J (1992) March's advanced organic chemistry. Wiley, New York
6. Ning L, Liao S, Liu X, Guo P, Zhang Z, Zhang H, Tong X (2018) J Catal 364:1–3
7. Fan C, Wang R, Kong P, Wang X, Wang J, Zhang X (2020) Catal Commun 140:106002
8. Jun G, Guoli F, Lan Y, Xinzhong C, Peng Z, Feng L (2017) Chem Cat Chem 9:1230–1241
9. Yajuan H, Yanzhu C, Shuru L, Hengquan Y (2012) J Phys Chem C 116:6512–6519
10. Ramakrishnan R, Kathiravan K, Sakthivel K, Sivakumar T (2016) RSC Adv 6:45907–45922
11. Chih Hsiang T, Mengze X, Pranaw K, Brian TG (2018) Catal Today 306:81–88
12. Singh S, Patel A, Prakashan P (2015) Appl Catal A 505:131–140
13. Li Y, Wang L, Yan R, Han J, Zhang S (2015) Catal Sci Technol 5:3682–3692
14. Wan X, Deng W, Zhang Q, Wang Y (2014) Catal Today 233:147–154
15. Suzuki K, Yamaguchi T, Matsushita K, Iitsuka C, Miura J, Akaogi T, Ishida H (2013) ACS Catal 3:1845–1849
16. Sanny V, Deepak V, Anil SK, Suman JL (2015) Appl Catal A 489:17–23
17. Yasukawa T, Yang X, Kobayashi S (2018) Org Lett 20:5772–5776
18. Xie J, Kammert JD, Kaylor N, Zheng JW, Choi E, Pham HN, Sang X, Stavitski E, Attenkofer K, Unocic RR, Datye AK, Davis RJ (2018) ACS Catal 8:3875–3884
19. Cui X, Li Y, Bachmann S, Scalone M, Surkus AE, Junge K, Topf C, Beller M (2015) J Am Chem Soc 137:10652–10658
20. Su H, Zhang KX, Zhang B, Wang HH, Yu QY, Li XH, Antonietti M, Shen JS (2017) J Am Chem Soc 139:811–818
21. Feng Y, Jia W, Yan GH, Zeng XH, Sperry J, Xu BB, Sun Y, Tang X, Lei TZ, Lin L (2020) J Catal 381:811–818
22. Eisenberg D, Slot TK, Rothenberg G (2018) ACS Catal 8:8618–8629
23. Slot TK, Eisenberg D, Rothenberg G (2018) Chem Cat Chem 10:2119–2124
24. Astrakova TV, Sobolev VI, Koltunov KY (2020) Catal Commun 137:105952
25. Cheng TY, Yu H, Peng F, Wang HG, Zhang BS, Su DS (2016) Catal Sci Technol 6:1007–1015
26. Jagadeesh RV, Junge H, Pohl MM, Radnik J, Bruckner A, Beller M (2013) J Am Chem Soc 135:10776–10782

27. Tang C, Surkus AE, Chen F, Pohl MM, Agostini G, Schneider M, Junge H, Beller M (2017) Angew Chem Int Ed 56:16616–16620

28. Wang X, Zhou J, Fu H, Li W, Fan X, Xin G, Zheng J, Li X (2014) J Mater Chem A 4:14064–14070

29. Li X, Jiang Q, Dou S, Deng L, Huo J, Wang S (2016) J Mater Chem A 4:15836–15840

30. Zheng W, Jiang X, Wang X, Kaneti YV, Chen Y, Liu J, Jiang JS, Yamauchi Y, Hu M (2017) Angew Chem Int Ed 56:8435–8440

31. Jiewei L, Lianfen C, Hao C, Jianyong Z, Li Z, Cheng Yong S (2014) Chem Soc Rev 43:6011–6061

32. Chen L, Chen H, Luque R, Li Y (2014) Chem Sci 5:3708–3714

33. Sun CY, To WP, Wang XL, Chan KT, Su ZM, Che CM (2015) Chem Sci 6:7105–7111

34. Gong YN, Ouyang T, He CT, Lu TB (2016) Chem Sci 7:1070–1075

35. Adeel CH, Nazir A, Hussein YA, Laypkovc A, Francis V (2015) Chem Soc Rev 44:6804–6849

36. Huang YB, Liang J, Wang XS, Cao R (2017) Chem Soc Rev 46:126–157

37. Xuning L, Xiang H, Shibo X, Shu M, Jie D, Weizheng C, Song L, Xiaoli Y, Hongbin Y, Jiajian G, Junhu W, Yanqiang H, Tao Z, Bin L (2018) J Am Chem Soc 140:12469–12475

38. Huirong C, Kui S, Junying C, Xiaodong C, Yingwei L (2017) J Mater Chem A 5:9937–9945

39. Ming Z, Chaohai W, Chao L, Rui L, Jiansheng L, Xiuyun S, Jinyou S, Weiqin H, Lianjun W (2018) J Mater Chem A 6:11226–11235

40. Feng J, Hailing G, Lei Z, Junjuan L, Yongming C, Svetlana M, Chenguang L (2019) Microporous Mesoporous Mater 276:98–106

41. Guowu Z, Hua Chun Z (2017) ACS Catal 7:7509–7519

42. Guihao Z, Dingxin L, Jianyong Z (2018) J Mater Chem A 6:1887–1899

43. Guangli Y, Jian S, Faheem M, Pengyuan W, Guangshan Z (2014) RSC Adv 4:38804–38811

44. Wei Z, Hongli L, Cuihua B, Shijun L, Yingwei L (2015) ACS Catal 5:1850–1856

45. Yu Xiao Z, Yu Zhen C, Lina C, Junling L, Hai Long J (2015) Chem Commun 51:8292–8295

46. Sun KK, Chen SJ, Li ZL, Lu GP, Cai C (2019) Green Chem 21:1602–1608

47. Feng Y, Jia W, Yan G, Zeng X, Sperry J, Xu B, Sun Y, Tang X, Lei T, Lin L (2020) J Catal 381:570–578

48. Alireza A, Mohammad S, Mahnaz N, Shokoofeh G (2017) J Mol Struct 1133:458–463

49. Xu Y, Li B, Zheng S, Wu P, Zhan J, Xue H, Xu Q, Pang H (2018) J Mater Chem A 6:22070–22076

50. Chao L, Taiqiang C, Weijing X, Xiaobing L, Likun P, Qun C, Bingwen H (2015) J Mater Chem A 3:5585–5591

51. Tao J, Tong ML, Chen XM (2000). J Chem Soc Dalton Trans. https://doi.org/10.1039/b005438k

52. Xu H (2008) Acta Cryst E64:m103

53. Kathiravan M, Thirusangumurugan S, Manzar S, Ahmad AS, Marga PM, Matthias B, Rajenahally JV (2018) Chem Sci 9:8553–8560

54. Heejun P, Sojin O, Sujeong L, Sora C, Moonhyun O (2019) Appl Catal B 246:322–329

55. Li W, Geng W, Liu L, Shang Q, Liu L, Kong X (2020) Sustain Energy Fuels 4:2043–2054

56. Wang Z, Xiao S, Zhu Z, Long X, Zheng X, Lu X, Yang S (2015) ACS Appl Mater Interfaces 7(7):4048–4055

57. Liu Y, Jiang H, Zhu Y, Yang X, Li C (2016) J Mater Chem A 4:1694–1701

58. Liua Y, Wanga C, Jua S, Lia M, Yuana A, Zhu G (2020) Prog Nat Sci Mater 30:185–191

59. Wang T, Ma H, Liu X, Luo Y, Zhang S, Sun Y, Wang X, Gao J, Xu J (2019) Chem Asian J 14:1515–1522

60. Bai C, Li A, Yao X, Liu H, Li Y (2016) Green Chem 18:1061–1069

61. Liu M, Zhang H, Wang J, Zhao G, Liu D (2020) React Kinet Mech Catal 129:865–881

62. Vineeta P, Amer NA, Ahmed A, Brigitte S, Pascal R, Rabah B, Suman JL (2015) RSC Adv 5:88567–88573

63. Hui S, Ke ZX, Bing Z, Hong WH, Qiu YY, Xin LH, Markus A, Jie CS (2017) J Am Chem Soc 139:811–818

64. Rui T, Lu GP, Zhao X, Chen Z (2021) Chin Chem Lett 32:685–690

65. Salazar A, Hunemorder P, Rabeah J, Quade A, Jagadeesh RV, Mejia E (2019) ACS Sustain Chem Eng 7:12061–12068

66. Zhou C, Tan Z, Jiang H, Zhang M (2018) Green Chem 20:1992–1997

67. Jiang BL, Lin Y, Wang ML, Liu DS, Xu BH, Zhang SJ (2019) Org Chem Front 6:801–807